Microfluid Nanofluid (2012) 13:345–352
DOI 10.1007/s10404-012-0957-z

RESEARCH PAPER

Implantable microfluidic and electronic systems for insect flight manipulation

Aram J. Chung · Bernardo Cordovez · Nipun Jasuja · Daniel J. Lee · Xinyu Toby Huang · David Erickson

Received: 1 January 2012 / Accepted: 16 February 2012 / Published online: 3 March 2012

Abstract Insect micro air vehicles represent a promising alternative to traditional small scale aircraft because they combine the enhanced energy storage and maneuverability of living insects with the controllability offered by microelectromechanical systems. These systems have been previously demonstrated, usually using either electrical (with implanted electrodes) or chemical (with implanted microfluidics) control schemes, but to date little work has been done on the creation of hybrid systems that use both these methods simultaneously. In this paper, we develop an integrated microsystem that uses both chemical and electrical methods to modulate the flight activity of *Manduca sexta* moths. The integration of two control schemes is essential because it could increase the number of achievable flight routines and duration. The electrical component of the system initiates and maintains flight by applying electrical pulses to an antenna lobe and an implanted drug delivery component modulates flight output power by administering a neurotransmitter dose to the central nervous system. Flight duration results acquired with this system are compared with those obtained from direct mechanical stimulation. We demonstrate that the electrical stimulation provides as much as 35-fold enhancement in flight duration with respect to mechanical agitation and that a 50% mean flight power output reduction can be achieved with the proper neurotransmitter dose.

Keywords Microfluidics · Drug delivery · Insect cyborg · *Manduca Sexta* moth flight control

1 Introduction

The downscaling of traditional air vehicles (Wootton 2000) presents severe challenges. Most prominently, wing size reduction compromises vehicle aerodynamics and makes a flapping type motion necessary in order to lift an aircraft body. One way this problem has been addressed in the past is by using microelectromechanical system (MEMS) technology (Tanaka 2007) to generate small flying robotic systems with biomimetic (Franz and Mallot 2000) characteristics. An example of this is the flapping *Diptera* robots reported by Wood (2008). Such systems however experience significant power constraints since storage capacity scales with the volume of the carrier, making it difficult to power the electrical components for extended periods. Insects, on the other hand, are aerodynamically efficient (Ellington 1984; Pesavento and Wang 2009) and offer superior flight endurance, but attempts to train and control them directly have proved challenging (Helm 2005).

One way to address this dichotomy is through the development of systems that take advantage of the energy storage and flight capabilities of living insects with the precise control enabled by modern MEMS technology. These systems are of significant technological interest

A. J. Chung and B. Cordovez contributed equally to this work.

Electronic supplementary material The online version of this article (doi:10.1007/s10404-012-0957-z) contains supplementary material, which is available to authorized users.

A. J. Chung · B. Cordovez · N. Jasuja · D. J. Lee · D. Erickson (✉)
Sibley School of Mechanical and Aerospace Engineering, Cornell University, 240 Upson Hall, Ithaca, NY 14853, USA
e-mail: de54@cornell.edu

X. T. Huang
Department of Entomology, Cornell University, Ithaca, NY 14853, USA

(Weinberger 2008) due to their applicability to remote surveillance (Lian et al. 2003) and power harvesting (Jeon et al. 2005; Wickenheiser et al. 2010). The dominant paradigm for insect flight manipulation is based on electrical control of neuromuscular activity (Bozkurt et al. 2009b). Aerodynamic operations including liftoff, yaw control and landing have been demonstrated by Bozkurt et al. (2009c) in *Manduca sexta* moths. Similar operations were performed by Sato et al. (2009) with *Cotinis texana* beetles using wireless DC pulses applied to neuromuscular centers demonstrating free flying up to 30 min. Tsang et al. (2010) demonstrated flight steering in *M. sextae* by controlling their abdominal orientation using a flexible electrode ring attached to the nerve cord. However, the achievable flight time is relatively short due to the lack of a lightweight and high-density power source. On the other hand, microsystems which use chemical control have also been developed. For example, Chung and Erickson (2009) induced a reversible chemical paralysis in a tethered *M. sexta* moth via an implantable microfluidic chip that released various neurotransmitter solutions. Chemical methods, while not as rapid, have the advantage of enabling longer term behavior (such as dormant periods) without the need for continuous external power.

A system that harnesses the maneuverability offered by the electrical approach with the speed control and physiological access enabled by chemistry could increase the number of achievable flight routines. Toward this end, in this paper we demonstrate the system integration of chemical and electrical methods for modulating the flight activity of *M. sexta* moths. To analyze the flight behavior, we performed a series of tethered experiments which measure changes in flight output power for different neurotransmitter doses subject to continuous electrical pulse stimulation. The results are used to create a wireless hybrid system that enables tetherless hybrid flight control compared with direct mechanical stimulation which is used as a baseline. We focus here on developing the hybrid flight mechanism rather than device miniaturization as this has already been demonstrated (Sato et al. 2009; Tsang et al. 2010; Bozkurt et al. 2009c).

2 Materials and methods

2.1 Microfabrication

The drug delivery system consists of three subcomponents. The first is a silicon layer containing a microwell with a suspended upper electrode through which fluids are ejected, a 3D printed acrylic channel coated with Parylene which contains the dose, and a bottom gold coated Pyrex substrate which serves as the counter electrode. The top silicon component was devised using the method established by Chung and Erickson (2009), in which LPCVD silicon nitride is deposited on both sides of a <100> n-doped silicon wafer. The backside was patterned to define the well location, followed by gold deposition on the top side. The wells were then etched by immersing the wafer in potassium hydroxide (KOH) overnight and the remaining silicon nitride underneath the gold membrane was removed through reactive ion etching. This left a 100 μm by 100 μm square suspended gold membrane. A photoactive polyimide layer was spun and patterned on the top of the device to reduce electrical contact outside of the suspended gold membrane. One millimeter tall acrylic channels were defined and cleaned with a sodium hydroxide (NaOH) solution, followed by a Parylene deposition to ensure impermeability to water. The three subcomponents were then assembled and sealed using biocompatible glue (Loctite® 454: ISO 10993, Henkel). The assembled device was then subjected to oxygen plasma cleaning, followed by fluidic loading from the backside and sealing using biocompatible wax (Butler GUM, Sunstar).

2.2 Implantation process

All relevant animal care and use guidelines were followed in this study. In this study, we use *M. sexta* moths as our model species due to its large body mass (~2 g) and a wingspan of 10 cm that are compatible with the microfluidic device dimension. The microfluidic chips were implanted in adult moths 2 days after emerging from the pupal stage. Prior to the surgery, the moths were placed on an ice platform for approximately 10 min to lower their internal body temperature and to minimize movement. With a sterilized scalpel, a portion of the dorsal exoskeleton was removed and the chip was gently pushed in approximately 3 mm into the thorax near the dorso-longitudinal flight muscles without removing any extra muscles. After gently inserting the device into the thorax, the wound was sealed using Loctite 454. This step was followed by the thin electrode implantation, which is gently inserted next to antennal lobe and sealed with the same biocompatible glue.

2.3 Displacement angle measurement and analysis

A thin wire leash was used to tether the moth's head and thorax to the swinging arm during the image tracking experiments. 10 μl solution volumes were used for all injections. The displacement angle was evaluated using a customized MATLAB code based on Hedrick et al.'s (2008) previous work. To track the insects' displacement in 3D tetherless flight, a reverse GPS system employing 24 VICON cameras was used to track IR reflecting balls attached to the helium balloon.

3 Results and discussion

3.1 Flight power/speed analysis of combined chemical and electrical modalities

In this first section, we analyze the flight response of *M. sextae* to simultaneous chemical and electrical stimulation. To characterize thrust, speed and flight power, moths were tethered to a hinged beam as shown in Fig. 1a. The displacement angle (θ) was measured and analyzed for moths that had been injected with solutions containing different concentrations of L-glutamic acid (LGA) neurotransmitters and 10 mM phosphate buffered saline (PBS) buffer solution which served as a negative control. LGA was chosen based on our previous work (Chung and Erickson 2009) where we have performed series of direct chemical injection experiments to gauge their effectiveness in generating the desired physiological responses. LGA tended to slow down or reversibly paralyze the insect with a small volume (as small as 5 µl) by acting on the neuronal receptors, neuronal ion channels or synaptic membrane (Chung and Erickson 2009; Rash and Hodgson 2002). The chemical injection was made using microliter syringe (NanoFilTM, World Precision Instrument). After injection, insects are stimulated into flight by supplying a sequence of 3 V, 25 Hz DC pulses with a 50% duty cycle for 0.5 s followed by a 1 s pause. 3 V was set same as the battery output though higher voltage may cause irreversible tissue damage. Bozkurt et al. (2008) reported that lower voltage (0.9 V) with similar frequency electrical shocking scheme is effective for flight muscle activation. In order to minimize unnecessary tissue damage, we programed three different shocking strategies depending on moth's flight capability as shown in Fig. S2. These pulses are applied between an electrode implanted near the antennal lobe and a common ground implanted in the dorsal thorax (Fig. 1a). These electrical pulses tended to stun the moth when initially applied, but resulted in strong flight behavior during the off cycle (see Movie S1). The electrical stimulation can maintain continuous flight activity and the role of the injected chemical is to throttle flight speed by overstimulating the moth's central nervous

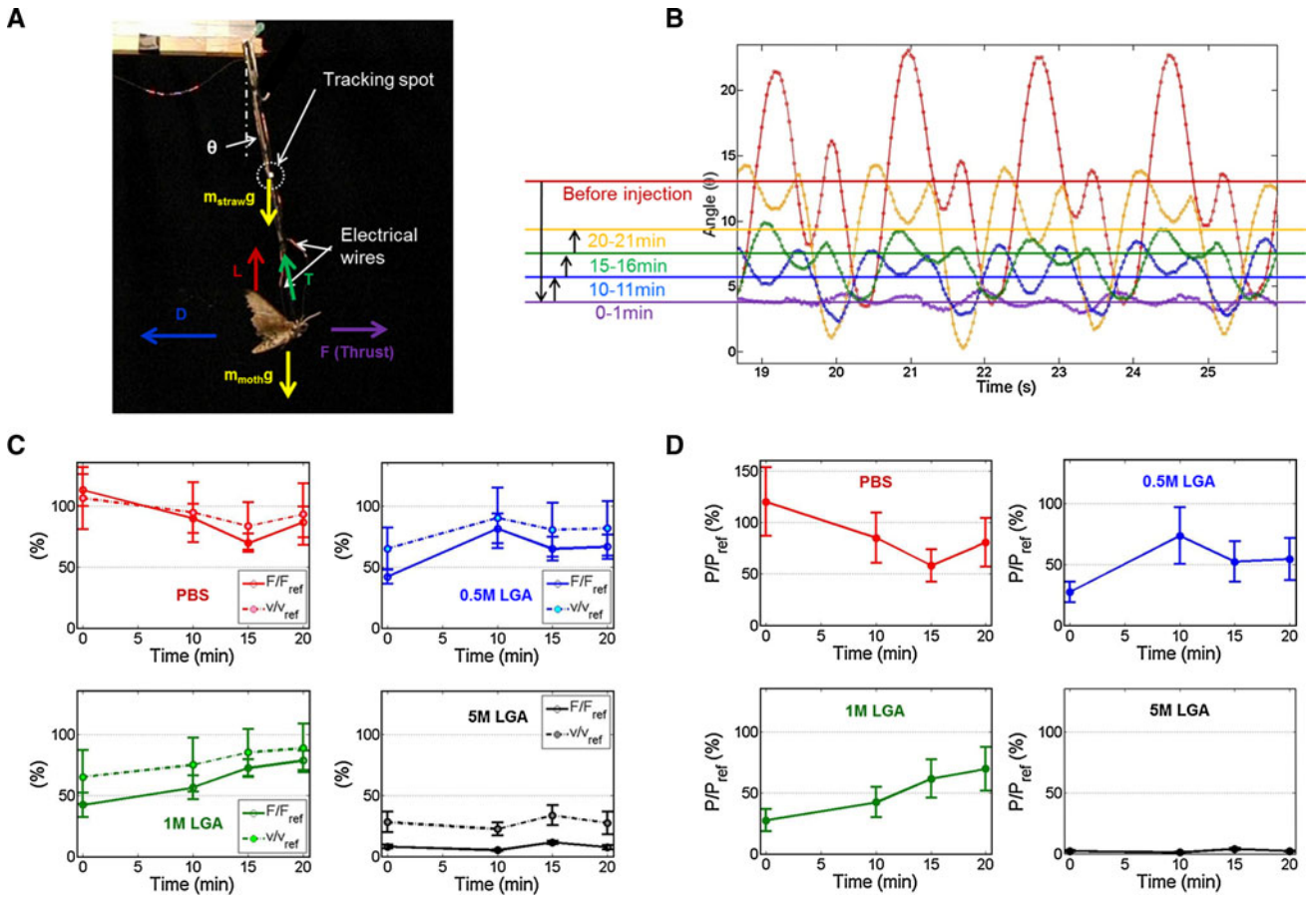

Fig. 1 Combined electrical and chemical modulation of insect flight power and speed. **a** Experimental setup showing moth attached to hinged solid beam (see Movie S1). **b** Flight angle before (*red*) and after 0.5 M L-glutamic acid (LGA) injection. c Flight velocity and thrust response following injection of different concentrations of LGA. **d** Flight power output following injection of different concentrations of LGA. The *error bars* represent standard error of the mean (color figure online)

system (Skinner et al. 1991). Figure 1b shows a sample experiment following manual injection of 10 µl of 0.5 M LGA solution.

To translate angle data into flight thrust, the simple moment balance shown below was used, the details of which are provided in the supplementary information (see Fig. S1).

$$F = g \tan \theta (m_{\text{straw}}/2 + m_{\text{moth}}), \quad (1)$$

The supplementary information also explains how the thrust data can also be converted to velocity and power output differences. The thrust and velocity characteristics of moths subjected to different concentrations of LGA are shown in Fig. 1c, and all values are normalized to the prior to injection state (denoted with the subscript "ref" in Fig. 1c, d). The thrust and velocity values 1 min after the injection of PBS (negative control) are higher compared to those obtained before injection. This is because inserting and withdrawing of the needle irritates the insects, and PBS does not drastically reduce flight capacity. For 1 and 0.5 M LGA solutions, moths fly on average at 22% below their pre-injection flight speed (Fig. 1c) for the first 20 min, with a gradual speed increase as the solution is metabolized. The flight power output is shown in Fig. 1d. 0.5 and 1 M LGA solutions result in rapid drop in output power which is regained to approximately 50% of the reference value within 10 min. Those subjected to 5 M doses regain half of their activity 1.5 h later. Long-term reduction in flight speed can be useful for applications such as remote surveillance (Lian et al. 2003). It is worth noting that the recovery time is approximately twofold quicker compared to our previous work (Chung and Erickson 2009) where no electrical stimulation was used. In addition to the functions demonstrated here, chemical injection could also offer additional capabilities. For example, different chemicals have been used to promote growth (Ziegler and Schulz 1986; Ziegler 1991) or to induce characteristic flight patterns (Claassen and Kammer 1986; Johnston and Levine 1996) in *M. sexta* moths.

3.2 Wireless hybrid system for insect flight modulation

We now construct and test a wireless system based on the electrical and chemical hybrid technique demonstrated above. The full scale system is shown in Fig. 2b and illustrated schematically in Fig. 2a for clarity. Movie S2 is an animated video that illustrates the hybrid stimulation process. For the integrated system, a commercial wireless microcontroller (TI eZ430) with multiple independent electrical output ports is used to trigger both the electrical

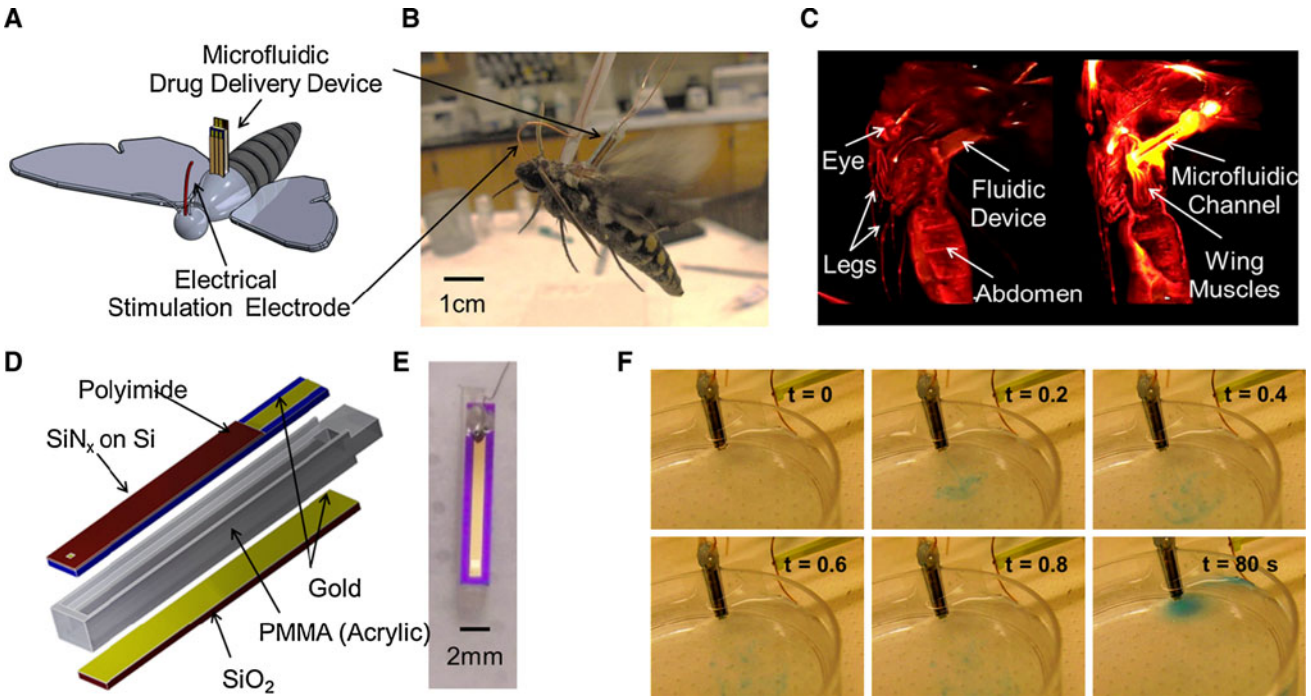

Fig. 2 Wireless hybrid system for *Manduca sexta* flight control. **a** Schematic of moth showing both microfluidic chip, which is implanted in dorsal thorax, and the copper wire used for electrical stimulation, implanted in the antennal lobe (see Movie S2 for interactive version). **b** Insect showing implanted microfluidic chip and electrode. **c** 3D Computed tomography (CT) image of fluidic chip implanted into dorsal thorax (also available as Movie S4). **d** Fluidic chip subcomponent assembly in exploded view and **e** actual fluidic chip. **f** Time lapse of images showing sample ejection sequence of 5 M L-glutamic acid (LGA) solution into 10 mM PBS solution (see Movie S3)

stimuli and the actuation of the microfluidic chip (see Fig. S1). The microfluidic chip (Fig. 2d–f) is implanted in the moth's dorsal thorax and uses an electrochemical pumping procedure that was previously demonstrated by Chung et al. (2009) where we have investigated how the insertion of the device affected moths' flight capability. Note that the dimension of the microfluidic chip used in this study is approximately half the volume as compared to the previous design. With regard to the ejection mechanism, chlorine ions in the buffer react with the capping gold membrane on top of the fluidic chip thereby dissolving it. In addition, water electrolysis releases gas which builds up the pressure in the enclosed chamber, leading to mechanical failure of the capping membrane and release of the contents. The microcontroller has a standard output of 3 V, so the anode of the microfluidic chip was connected to a custom designed 34 V DC to DC converter to increase the reaction rate. The bottom electrode of the fluidic chip is connected to the universal ground. This version of the chip is 4 times smaller than its predecessor (Chung et al. 2009) while still capable of carrying the same volumetric payload. This was achieved by reducing the lithographic pattern dimensions as well as implementing a custom 3D printed acrylic channel to hold the chemical payload (see "Materials and methods" for more details on fabrication). Figure 2f is a time-lapse image showing the fluidic ejection of 5 M LGA solution (also see Movie S3). The enclosed solution bursts out of the device at a speed of nearly 10 cm/s and the majority of the fluidic contents are ejected by the 80 s mark. The chemical ejection mechanism from the microfluidic chip may cause additional side effects (i.e. ohmic heating generation, created gases by electrolysis, and ejection process). Although we have not fully characterized, no observable difference was found for manual and device injections. Injection of PBS (zero LGA concentration as a negative control) through both microfluidic device and syringe injection slowed down the moth as in our previous work (Chung and Erickson 2009) but not nearly to the extent that the paralysis chemicals did. In both this and our previous paper (Chung and Erickson 2009), recovery to very near the initial flight power has been recorded indicating that there is very little permanent damage. In addition, the much of unfavorable effects can be avoided by reducing the DC to DC converter output voltage for further studies. Electrical stimulation was achieved by implanting a thin wire electrode in the moth's antennal lobe (Fig. 2a, b) and connecting it to a secondary output port of the wireless microcontroller. To facilitate our experiments, we use a 6 l helium balloon to support the additional weight of the communication payload (6 g), however, it has been already demonstrated that low weight electrical communication systems (Bozkurt et al. 2009a; Sato et al. 2009; Tsang et al. 2010) are possible, and with future integration with one of these it may be possible to demonstrate untethered and free flying in the absence of balloon. To assess the invasiveness of our microfluidic and electrical implants, Fig. 2c and Movie S4 show a 3D CT scan following implantation. We note that the chip penetrated approximately 3 mm into the thorax, bringing the chemical payload close to both the central nervous system and the main circulatory system for effective drug dispersal.

The operation and characterization of the system is shown in Fig. 3 and in Movie S5. The insect is brought from rest (Fig. 3a) into takeoff (Fig. 3b) by supplying the same pulse sequence used in Figs. 1 and 2 and in Movie S1. After 30 s of sustained flight (Fig. 3c), the microfluidic chip was actuated, releasing the 5 M solution of LGA. The insect responds by first decelerating for about 20 s until it reaches full paralysis (Fig. 3c). The DC pulse routine was suspended during chemical release to prohibit interference between the two signals but resumed immediately after dosing was complete. The success rate from takeoff to full paralysis was 50% with a sample size of 20. To track accurately the moth's displacement and flight speed changes during flight, we used a VICON tracking system (VICON, Oxford, UK). The length, height, and width of the working domain were 10, 1.5, and 6 m, respectively (see Fig. S3). Twenty-four infrared cameras were used to measure the flight path with a 60 Hz sampling rate. Two representative flight trajectories of full hybrid tests are presented in Fig. 3d, illustrating the three stages of flight: The red region denotes sustained flight under electrical stimulation (average flight speed 10 cm/s), followed by the drug delivery stage shown in green which captures the transition from stimulation to deceleration, and finally deceleration (blue) due to chemical overstimulation. Moths have different starting points because they were initially resting at different heights. The time to reach the onset of paralysis from the chemical ejection is within 5 s for both cases. Figure 3e shows the vertical displacement and its corresponding speed as a function of time. Both trends in Fig. 3e also show how the moths reach a standstill once they hit the ground.

3.3 Comparison of electrical and mechanical flight duration enhancement modalities

In nature *M. sexta* moths tend to fly sporadically, a few times a day and in a manner that is very sensitive to the environmental conditions (McCrea and Heath 1971). In practice it becomes necessary then to override their native behavior to achieve predictable flight duration. Previously we demonstrated that direct mechanical stimulation can also be used to enhance flight duration (Chung and Erickson 2009). Although it is more difficult to construct an insect portable mechanical stimulation system, than it is for

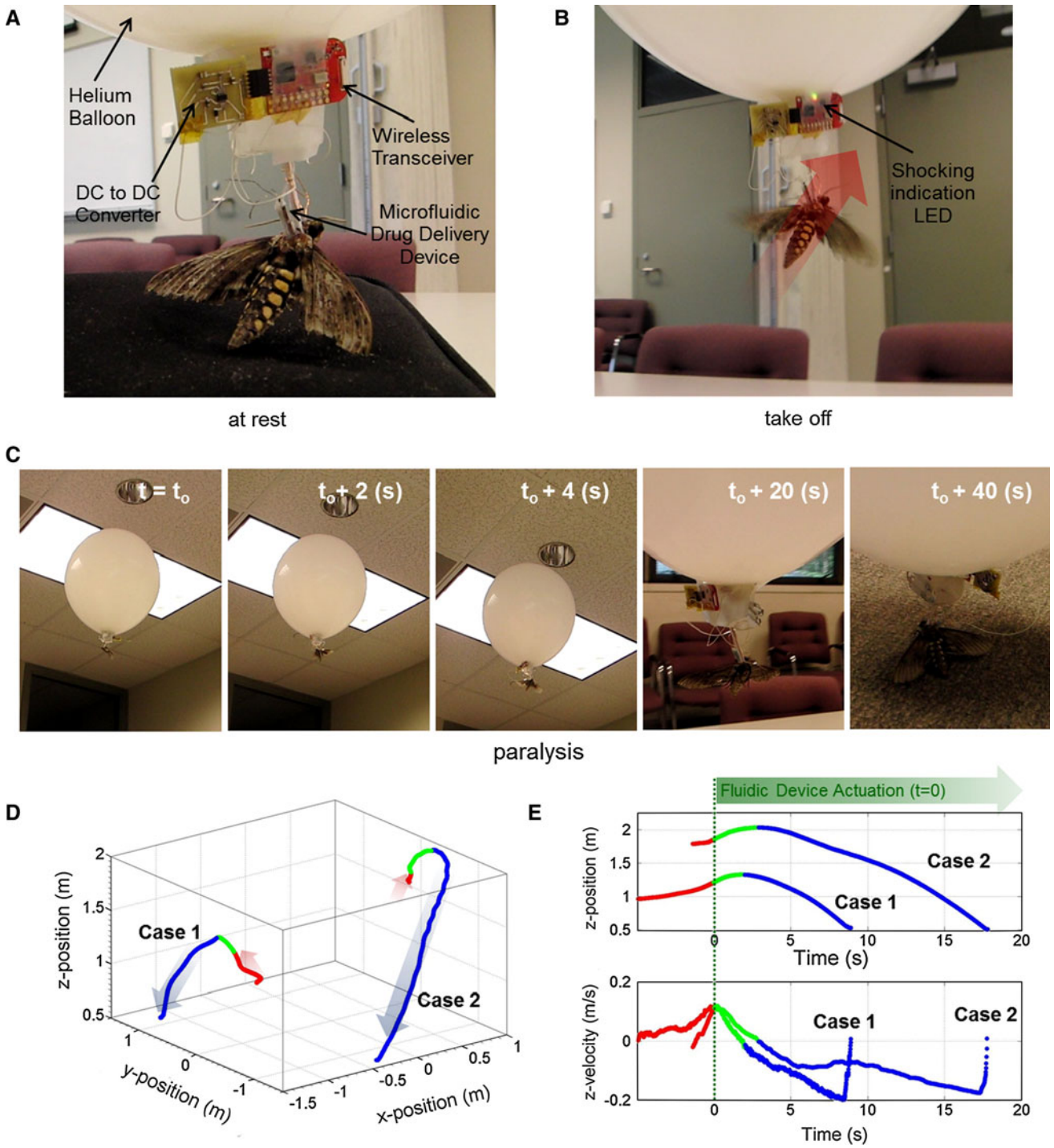

Fig. 3 Wireless hybrid flight operation and flight tracking. **a** Moth at rest. **b** Electrically stimulated takeoff. **c** Time-lapse images showing moth subjected to electrical stimulation followed by chemically induced paralysis. **d** Two representative cases of insect trajectories where the *red* bands denote flight under electrical stimulation, *green* during the drug delivery stage and *blue* during the deceleration due to chemical overstimulation (total sample size is 50 with a 50% success rate). **e** Vertical displacement and speed as a function of time. Insects speed up during electrical stimulation (*red*), are subjected to the chemical release (*green*) and decelerate (*blue*) due to chemical overstimulation (see Movie S5) (color figure online)

the electrical and chemical techniques demonstrated above, it is worthwhile to quantitatively determine which stimulation technique is better at promoting flight duration.

The results of our experiments comparing flight duration for these modalities are shown in Fig. 4 and Movies S1 and S6. Mechanical stimulation experiments were conducted

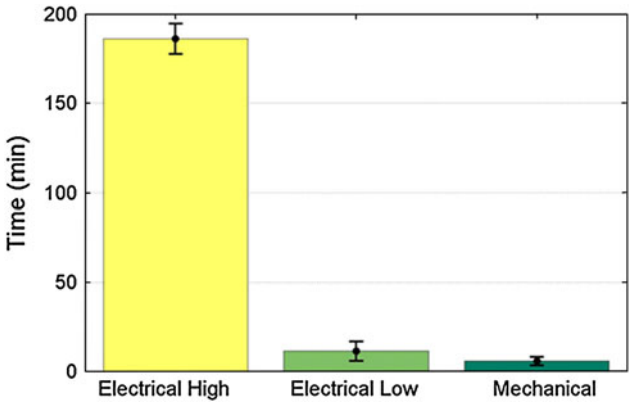

Fig. 4 Comparison of mechanical and electrical flight duration enhancement techniques (see Movies S1 and S6 for electrical and mechanical stimulation, respectively, and Fig. S4 for experimental setup). Comparison of electrical and mechanical enhancements in flight endurance showing both high and low electrical response groups. The *error bars* represent standard error of the mean

without tampering with moth internal physiology (which does occur with both electrical and chemical implants), by rubbing a spinning cotton swab on the moth's head as shown in Fig. S4 and Movie S6. The cotton swab is attached to a pulsed DC motor and operates at the same frequency and duty cycle as that of the electrical stimulation experiments described above. The criterion used in these experiments is that 10 s of no flapping activity is considered as a full stop and the end of a test. Moths subjected to mechanical stimulation flew for an average of 5 min as shown in Fig. 4. For electrical stimulation, data were collected using a similar apparatus to that shown in Fig. 1. It was observed that these insects responded in a bimodal way with one group tending to fly continuously for close to 3 h on average and the other which flew for 17 min on average. The reason for this bimodal response is not known, however, it was clear that the low flight endurance group were much more rapid to adapt to the presence of electrical stimulation. When compared to the mechanically stimulated group, the high flight endurance group exhibited a 35-fold enhancement in flight duration.

4 Conclusions

In summary, here we have demonstrated the use of simultaneous chemical and electrical modalities for modulating the flight activity of *M. sexta* moths. The optimal hybrid stimulation conditions were determined through series of tethered experiments and implemented on a wireless insect-borne system. The results were quantitatively analyzed by comparing them with baseline measurements using mechanical stimulation. It was shown that electrical stimulation can result in as much as 35-fold improvement (on average 3 h continuous flight) in flight duration and chemically induced neurotransmitters overdose could result in a recoverable 50% mean flight speed reduction. This combined modality could allow for a broader range of flight operations to be performed.

Acknowledgments The authors would like to thank J. Atchison for his contributions towards the boost converter design, Prof. M. Campbell and Prof. H. Kress-Gazit for access to the VICON system, M. Kalontarov for helpful discussions, Prof. H. Lipson for access to the 3D Acrylic Printer and Dr. M. Ozgur at MEMS Exchange. This work was supported by the DARPA Defense Sciences Office under the HI-MEMS program through the BTI for Plant Research. Distribution unlimited. The facilities used for this research include Cornell Nanoscale Science and Technology Facility (CNF), Nanobiotechnology Center (NBTC) at Cornell University.

References

Bozkurt A, Gilmour R, Stern D, Lal A (2008) MEMS based bioelectronic neuromuscular interfaces for insect cyborg flight control. In: Proceedings of the 21st IEEE International Conference on MEMS, pp 160–163

Bozkurt A, Gilmour RF, Lal A (2009a) Balloon-assisted flight of radio-controlled insect biobots. IEEE Trans Biomed Eng 56(9):2304–2307

Bozkurt A, Gilmour RF, Sinha A, Stern D, Lal A (2009b) Insect–machine interface based neurocybernetics. IEEE Trans Biomed Eng 56(6):1727–1733

Bozkurt A, Lal A, Gilmour R (2009c) Aerial and terrestrial locomotion control of lift assisted insect biobots. In: Proceedings of the IEEE Engineering in Medicine and Biology Society, pp 2058–2061

Chung AJ, Erickson D (2009) Engineering insect flight metabolics using immature stage implanted microfluidics. Lab Chip 9(5):669–676

Chung AJ, Huh Y, Erickson D (2009) A robust, electrochemically driven microwell drug delivery system for controlled vasopressin release. Biomed Microdevices 11(4):861–867

Claassen DE, Kammer AE (1986) Effects of octopamine, dopamine, and serotonin on production of flight motor output by thoracic ganglia of *Manduca Sexta*. J Neurobiol 17(1):1–14

Ellington CP (1984) The aerodynamics of hovering insect flight.1. the quasi-steady analysis. Philos Trans R Soc Lond Ser B Biol Sci 305(1122):1–15

Franz MO, Mallot HA (2000) Biomimetic robot navigation. Robot Auton Syst 30(1–2):133–153

Hedrick TL (2008) Software techniques for two- and three-dimensional kinematic measurements of biological and biomimetic systems. Bioinspir Biomim 3(3):034001–034006

Helm B (2005) Finding land mines by following a bee. Business Week

Jeon YB, Sood R, Jeong Jh, Kim SG (2005) MEMS power generator with transverse mode thin film PZT. Sens Actuators A 122(1):16–22

Johnston RM, Levine RB (1996) Crawling motor patterns induced by pilocarpine in isolated larval nerve cords of *Manduca sexta*. J Neurophysiol 76(5):3178–3195

Lian YS, Shyy W, Viieru D, Zhang BN (2003) Membrane wing aerodynamics for micro air vehicles. Prog Aerosp Sci 39(6–7):425–465

McCrea MJ, Heath JE (1971) Dependence of flight on temperature regulation in the moth *Manduca Sexta*. J Exp Biol 54(2):415–435

Pesavento U, Wang ZJ (2009) Flapping wing flight can save aerodynamic power compared to steady flight. Phys Rev Lett 103(11):118102

Rash LD, Hodgson WC (2002) Pharmacology and biochemistry of spider venoms. Toxicon 40(3):225–254

Sato H, Berry CW, Peeri Y, Baghoomian E, Casey BE, Lavella G, Vandenbrooks JM, Harrison JF, Maharbiz MM (2009) Remote radio control of insect flight. Front Integr Neurosci 3:24

Skinner WS, Dennis PA, Li JP, Summerfelt RM, Carney RL, Quistad GB (1991) Isolation and Identification of Paralytic Peptides from Hemolymph of the Lepidopteran Insects *Manduca Sexta*, *Spodoptera exigua*, and *Heliothis virescens*. J Biol Chem 266(20):12873–12877

Tanaka M (2007) An industrial and applied review of new MEMS devices features. Microelectron Eng 84(5–8):1341–1344. doi: 10.1016/j.mee.2007.01.232

Tsang WM, Stone AL, Aldworth ZN, Hildebrand JG, Daniel TL, Akinwande AI, Voldman J (2010) Flexible split-ring electrode for insect flight biasing using multisite neural stimulation. IEEE Trans Biomed Eng 57(7):1757–1764

Weinberger S (2008) Defence research: Still in the lead? Nature 451:390–393

Wickenheiser AM, Reissman T, Wu WJ, Garcia E (2010) Modeling the effects of electromechanical coupling on energy storage through piezoelectric energy harvesting. IEEE-ASME Trans Mechatron 15(3):400–411

Wood RJ (2008) The first takeoff of a biologically inspired at-scale robotic insect. IEEE Trans Robot 24(2):341–347

Wootton R (2000) Aerodynamics: From insects to microvehicles. Nature 403(6766):144–145

Ziegler R (1991) Changes in lipid and carbohydrate-metabolism during starvation in adult *Manduca sexta*. J Comp Physiol B Biochem Syst Environ Physiol 161(2):125–131

Ziegler R, Schulz M (1986) Regulation of carbohydrate-metabolism during flight in *Manduca sexta*. J Insect Physiol 32(12):997–1001